Enzyme Mechanisms

DOI: 10.1002/ange.200903407

Specificity and Mechanism of *Acinetobacter baumanii* Nicotinamidase: Implications for Activation of the Front-Line Tuberculosis Drug Pyrazinamide**

*Paul K. Fyfe, Vincenzo A. Rao, Aleksandra Zemla, Scott Cameron, and William N. Hunter**

Nicotinamidase (EC 3.5.1.19) catalyzes hydrolysis of nicotinamide to nicotinic acid and ammonia, an important reaction in the NAD^+ salvage pathway.[1] This activity has a fortuitous medical benefit since the *Mycobacterium tuberculosis* enzyme converts the nicotinamide analogue prodrug pyrazinamide into the bacteriostatic pyrazinoic acid,[2–4] hence the alternative name, pyrazinamidase (PncA). Pyrazinoic acid inhibits *M. tuberculosis* type I fatty acid synthase,[5] represses mycolic acid biosynthesis, and appears to affect membrane energetics and acidification of the cytoplasm.[4] It is active against semi-dormant tubercle *bacilli* and with rifampicin and isoniazid, forms the front-line tuberculosis treatment.[2,3] Though studies of PncA have revealed aspects of its structure and biochemical activity[6–9] there are no structural data on how the enzyme binds and processes physiological ligands. High-resolution crystal structures of *Acinetobacter baumanii* PncA (*Ab*PncA) complexed with nicotinic acid and pyrazinoic acid now provide direct evidence for the interactions that govern the specificity and mechanism, and of how a valued antibacterial agent is activated.

Recombinant *Ab*PncA was prepared, the dimeric, colorless enzyme was purified in high yield and its kinetic properties determined. With pyrazinamide as the substrate the following values were obtained; $K_M = 106.9\ \mu M$, $V_{max} = 62.8\ nmol\,min^{-1}$, $k_{cat.} = 3.1\ min^{-1}$, specific activity $132\ \mu M\,min^{-1}\,mg^{-1}$. These values are comparable to literature values, for example, the specific activity of *M. tuberculosis* PncA (*Mt*PncA) with pyrazinamide is $82\ \mu M\,min^{-1}\,mg^{-1}$.[8]

Two crystal forms (I and II) were obtained with nicotinic and pyrazinoic acid, respectively, and the structures determined. PncA is a divalent cation-dependent enzyme and activity has been reported with Fe^{2+}, Mn^{2+},[8] and Zn^{2+} ions.[6] As expected, metal ions were observed in the structures. Inductively coupled plasma-atomic emission spectrometry (ICP-OES) identified that recombinant *Ab*PncA contained Fe^{2+} and Zn^{2+} ions in an approximate 1:1 ratio with a trace of Mn^{2+} present. However, anomalous dispersion measurements are consistent with a higher occupancy of Zn^{2+} at the active site and the crystallographic models contain that cation. We refer to Zn^{2+} ions in discussion but judge it likely that *Ab*PncA functions in the presence of different divalent cations. (Experimental details, including enzyme activity and metal-ion identification, together with sequence alignments, and additional figures are given as Supporting Information Figure S1–S8).

Crystals were obtained in the presence of cacodylate buffer and form II shows dimethylarsinoyl-modified Cys159 in the active site, an artifact of crystallization (Supporting Information, Figure S1, S2). The steric hindrance of this modification precludes full occupancy of pyrazinoic acid such that the final refinement was performed with occupancy 0.8 for pyrazinoic acid, 0.2 for the modified cysteine. Crystal form I has two molecules, form II a single molecule in the asymmetric unit, respectively, with a root-mean-square deviation (r.m.s.d.) derived from least-squares fit of Cα atoms of these three molecules of 0.2 Å. The structures and the interactions formed by ligands within the active sites are essentially identical and we concentrate on form I, a 1.65 Å resolution structure with full occupancy ligand (Supporting Information, Figure S3). About 60% of residues form elements of secondary structure, these are eight α-helices and nine β-strands (Figure 1, and Supporting Information, Figure S4). The core of the subunit is a parallel β-sheet of strands 1, 2, 5–9. Three helices (α5, α6, α7) lie on one side of the sheet, with α2 placed against the other. A subdomain is placed at

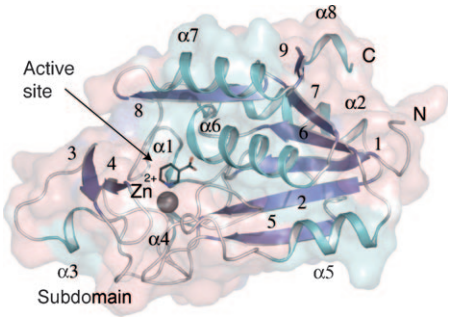

Figure 1. Ribbon diagram of the *Ab*PncA monomer and location of the active site. The Zn^{2+} ion is shown as a gray sphere, nicotinic acid as a stick model: black C, blue N, red O. Helices (cyan) are labeled and β-strands (blue) numbered. The terminal positions of the polypeptide are labeled N and C. Molecular images prepared with PyMol.[14]

[*] Dr. P. K. Fyfe, V. A. Rao, A. Zemla, Dr. S. Cameron, Prof. W. N. Hunter
Division of Biological Chemistry and Drug Discovery, College of Life Sciences,
University of Dundee, Dow Street, Dundee DD1 5EH (UK)
Fax: (+44) 1382-385764
E-mail: w.n.hunter@dundee.ac.uk

[**] Funded by the BBSRC [BBS/B/14434], The Wellcome Trust [082596 and 083481] and EC Seventh Framework Programme (FP7/2007-2013). We thank Lorna Eades of the University of Edinburgh, Mark Agacan, the Diamond Synchrotron Radiation Facility and the European Synchrotron Radiation facility for support.

Supporting information for this article is available on the WWW under http://dx.doi.org/10.1002/anie.200903407.

one end of the β-sheet and includes β3 and β4 and a single turn of helix, α3.

Gel filtration and analytical ultracentrifugation indicate that *Ab*PncA is a stable dimer in solution, approximate mass 47 kDa. The asymmetric unit of form I is a dimer (Supporting Information, Figure S5), with an interface of 900 Å^2, which is about 10% of the surface area of a subunit. In form II the crystallographic twofold axis generates the same dimer. The interactions that stabilize the dimer mainly involve residues on α5 and β5. The *Ab*PncA subunit resembles orthologues from *Pyrococcus horikoshii* (*Ph*PncA) and *Saccharomyces cerevisae* (*Sc*PncA).[6,7] Superpositions give r.m.s.d. values of 1.2 Å for the overlay of an *Ab*PncA subunit on either *Ph*PncA (44% sequence identity, 167 Cα atoms) or *Sc*PncA (33% identity, 191 Cα atoms).

The *Ab*PncA active site is between the core and the subdomain (Figure 1), and is formed by residues on β1, β2, the β4–α4 loop, β5, and the β6–α6 turn. It is buried and completely occluded from solvent by four polypeptide segments; the loops linking α3–β3, β5–α5, and β8–α9 together with strand β4. Numerous hydrophobic residues (discussed below) surround the active site and a gross conformational change is probably required to permit substrate binding or release of products.

The active site Cys159 is located at the N-terminus of α6 at one side of the active site with the Zn^{2+} ion positioned on the other side. The metal ion is held tightly in the *Ab*PncA active site as shown by activity being retained in the presence of 10 mM EDTA (data not shown). Octahedral coordination of Zn^{2+} ion involves Asp54 OD2, His56 NE2, and His89 NE2, two water molecules and nicotinic acid N5 (Figure 2). Cation–ligand distances range from 2.11 to 2.28 Å, consistent with data on Zn^{2+} ligand geometry.[10] A network of hydrogen bonds position the coordinating groups. One water molecule forms hydrogen bonds with Ser62 OG and Asp121 OD2, the other with Asp54 OD1 and Asp121 OD1. The coordinating

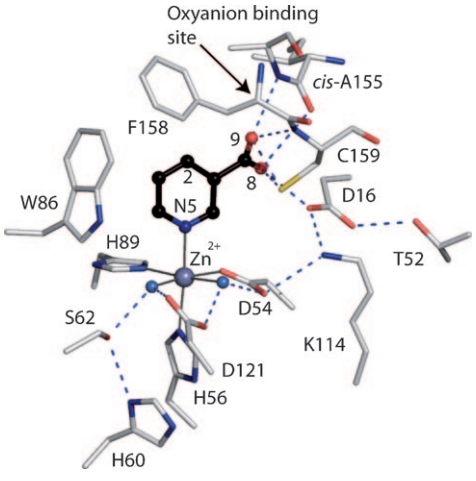

Figure 2. Active site of the nicotinic acid complex. The Zn^{2+} ion is a blue-gray sphere, thin lines mark coordination to amino acid side chains and two water molecules (marine spheres). Amino acids are in stick representation: C gray, N blue, O red, S yellow. Nicotinic acid is shown as a ball-and-stick model: C black, N blue, O red. Dashed lines represent potential hydrogen bonds.

His56 and His89 residues donate hydrogen bonds from ND1 to carbonyl groups of Gly115 and Pro87, respectively (data not shown). Nicotinic acid is tethered to the cation and positioned between five hydrophobic residues; Phe21, Leu27, Trp86, Tyr123, and Cys159 (Supporting Information, Figure S6). Trp86 NE1 and Tyr123 OH form a hydrogen bond to hold these residues in place over the ligand. A further six residues (Val29, Ile154, Ala155, Phe158, Ile184, and Leu186) stabilize the hydrophobic environment around the nicotinic acid and occlude the active site (Supporting Information, Figure S6). In the absence of a ligand, the Zn^{2+} coordination sphere is completed with a water as indicated in structures of *Ph*PncA and *Sc*PncA.[6,7] Nicotinic acid O8 and O9 are 2.5 and 2.6 Å, respectively, from Cys159 SG suggesting the presence of a bifurcated hydrogen bond. The next nearest functional group to Cys159 SG is Asp16 OD2 at a distance of 3.4 Å. O9 accepts hydrogen bonds donated from main-chain amides of *cis*-Ala155 and Cys159. Interaction with the *cis*-Ala155 carbonyl group suggests that O8 is a hydroxy group and that protonation of Asp16 OD2 may facilitate a second hydrogen bond (Supporting Information, Figure S7). Alternatively, O8 as hydroxy group or if protonated may participate in a bifurcated hydrogen bond with Asp16 and Ala155. Asp16, together with Asp54 and Lys114 form a cluster of interacting hydrophilic residues on one side of the ligand-binding site. Lys114 NZ donates hydrogen bonds to Asp16 OD1, Asp54 OD2, (Figure 2) and the main-chain carbonyl group of Tyr123 (not shown). The close proximity of Lys114 to Asp16 is likely to influence the pK_a value. The Asp16 carboxylate and main-chain amide groups form hydrogen bonds with Thr52 OG1 (Supporting Information, Figure S7), a pairing strictly conserved in PncA (Supporting Information, Figure S8).

Amidation involves either acidic or basic hydrolysis and the structures of the enzyme–product complex suggest that basic hydrolysis applies in PncA. Acid hydrolysis would involve nucleophilic water attacking the carbon of a protonated amide. The hydrophobic environment on one side of the amide and close interactions with functional groups on the other renders it difficult to envisage how water could be placed to attack C7. Nicotinic acid O9 accepts hydrogen bonds from two amides so protonation at O9 would destabilize the complex due to the proximity of the amides.

A more likely mechanism is indicated by a strictly conserved and essential Cys159,[6,8] on the polar side of the active site, ideally placed to attack the carbonyl carbon atom in a manner similar to that proposed for other enzymes, for example trypanothione synthetase amidase[11] and the nitrilase enzyme superfamily.[12] Nitrilases exploit a catalytic triad consisting of a reactive cysteine, a lysine, and a glutamate. The triad of PncA has a conservative difference with aspartate replacing glutamate.

We propose a four-stage mechanism (Figure 3). In stage I, substrate binds in the axial position displacing a water from the Zn^{2+} coordination sphere. The waters coordinating to equatorial sites of the metal ion are also held in position by hydrogen-bonding interactions to the enzyme (Figure 2), whereas the axial water lacks such a restraint. It is this water that vacates the coordination sphere as substrate binds.

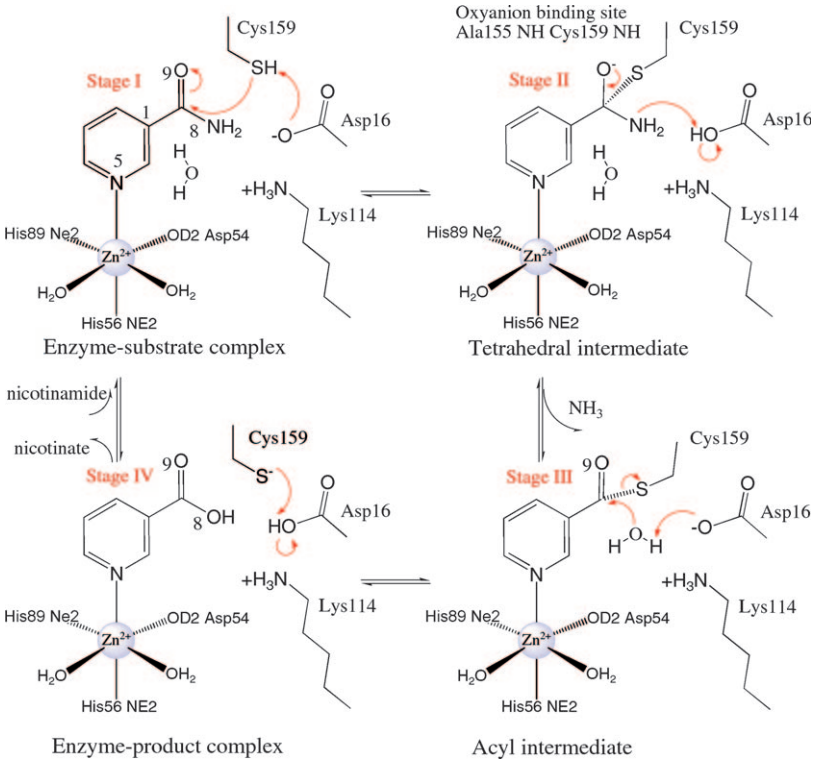

Figure 3. Proposed mechanism of nicotinamidase. see text for details.

This water may be prevented from exiting the active site by the hydrophobic lid covering the active site (Supporting Information, Figure S7). The displaced water, or an incoming water would preferentially bind to the hydrophilic side of the active site near Lys114. Proton abstraction by Asp16 would generate a Cys159 thiolate facilitating nucleophilic attack at C7. Two main-chain amides (*cis*-Ala155 and Cys159) form an oxyanion hole to support thiolate attack by stabilizing the resulting tetrahedral intermediate in a similar fashion to cysteine proteases.[13] Proton donation from Asp16 to N8 of the substrate would promote C–N bond cleavage and release of NH_3 as the tetrahedral intermediate collapses in stage II to give an acyl intermediate. Water activation by Asp16, whereby the amino acid is protonated, generates a nucleophilic hydroxy group to attack the acyl intermediate producing nicotinic acid (or pyrazinoic acid) and a thiolate in stage III. In stage IV, products are released and the thiolate accepts a proton from Asp16 to regenerate a thiol.

A previously proposed mechanism invoked a Zn^{2+}-coordinated hydroxy and an incoming water participating in catalysis:[6] First a hydroxy group directly attacks the acyl intermediate to replace the amino group, and then another incoming water coordinates to the Zn^{2+} ion as a hydroxy with a proton removed by the nearby aspartate to enable nucleophilic attack on the acyl intermediate. This mechanism appears unduly complicated with two rounds of metal-ion-directed water activation and is incompatible with our new structures. Activation of water to hydroxy groups by the strong Lewis acid that is four-coordinate Zn^{2+} ion is a commonly invoked feature of zinc-dependent enzymes. In PncA, the metal ion is six-coordinate and this would reduce the Lewis acid strength. In addition, as PncA catalysis is supported by different divalent cations this suggests that Lewis acid strength is less important than the structural role provided by octahedral coordination, precise placement of the substrate and an appropriate ligand exchange rate to support substrate binding with release of a water molecule. We therefore propose a simpler mechanism (Figure 3) with no requirement for the metal ion to activate water.

Recombinant *Mt*PncA produced in *Escherichia coli* is reported to carry a mixture of Fe^{2+} and Mn^{2+} ions and reconstitution of apoenzyme with these ions resulted in almost full recovery of activity, surprisingly reconstitution with Zn^{2+} did not.[8] Moreover, mutation of *Mt*PncA His56 to alanine led to almost complete loss of metal-ion binding and enzyme activity. These observations were taken to imply that His56 was directly involved in metal-ion binding and that *Mt*PncA binds ions in a different manner from *Ph*PncA.[8] *Mt*PncA His56 corresponds to *Ab*PncA His60, a residue that contributes significantly to the formation of the cation binding site by forming a hydrogen bond to Ser62 OG and positioning the serine to stabilize one of the waters that coordinates Zn^{2+} ion (Figure 2). His60 also stabilizes the coordinating His56 by van der Waals interactions and this histidine pair is strictly conserved in PncA sequences. Indeed, 16 of the 20 amino acids involved in cation coordination, substrate recognition, and catalysis are strictly conserved between *Ab*PncA and *Mt*PncA, with a further three involving conservative substitutions (Supporting Information, Figure S8). This suggests that all PncA enzymes share metal-ion binding properties and mechanism of action. Structural data on recombinant enzyme and metal-ion analysis of native *Mt*PncA would further clarify this.

Over 60 *M. tuberculosis* strains display pyrazinamide resistance owing to *pnca* gene mutations and more than 50% of these localize changes to three short polypeptide sections.[4,8] In *Ab*PncA these correspond to β1–α1, α3–β3 segments, and α6, near the active site and with residues important for substrate binding and catalysis. Of note is the strictly conserved Lys114 residue. Pyrazinamide-resistant mutants of *M. tuberculosis* containing a lysine–threonine change in this position have been identified.[9] This change may disrupt the hydrophilic environment required to allow for the exploitation of water in the proposed mechanism and/or would fail to align Asp16 for catalysis.

In summary, the precise nature of how nicotinic acid, and pyrazinoic acid bind *Ab*PncA casts doubt on a previously proposed mechanism, which was based on modeling substrate in a manner that did not include direct interaction with the Zn^{2+} ion. Our data reveal that substrate recognition involves interaction between the Zn^{2+} ion and the pyridyl nitrogen atom and that the position of functional groups has allowed us to propose a new mechanism for nicotinamidase activity and

one which likely applies to the activation of the anti-tuberculosis drug pyrazinamide.

Received: June 23, 2009
Revised: August 24, 2009
Published online: October 26, 2009

Keywords: drug discovery · enzymes · mechanisms · tuberculosis · zinc

[1] G. Magni, A. Amici, M. Emanuelli, N. Raffaelli, S. Ruggieri, *Adv. Enzymol. Relat. Areas Mol. Biol.* **1999**, *73*, 35 – 82.
[2] R. Shi, N. Itagaki, I. Sugawara, *Mini. Rev. Med. Chem.* **2007**, *7*, 1177 – 1185.
[3] P. Singh, A. K. Mishra, S. K. Malonia, D. S. Chauhan, V. D. Sharma, K. Venkatesan, V. M. Katoch, *J. Commun. Dis.* **2006**, *38*, 288 – 298.
[4] Y. Zhang, D. Mitchison, *Int. J. Tuberc. Lung Dis.* **2003**, *7*, 6 – 21.
[5] O. Zimhony, J. S. Cox, J. T. Welch, C. Vilchèze, W. R. Jacobs, *Nat. Med.* **2000**, *6*, 1043 – 1047.
[6] X. Du, W. Wang, R. Kim, H. Yakota, H. Nguyen, S. H. Kim, *Biochemistry* **2001**, *40*, 14166 – 14172.
[7] G. Hu, A. B. Taylor, L. McAlister-Henn, P. J. Hart, *Biochem. Biophys.* **2007**, *461*, 66 – 75.
[8] H. Zhang, J. Y. Deng, L. J. Bi, Y. F. Zhou, Z. P. Zhang, C. G. Zhang, Y. Zhang, X. E. Zhang, *FEBS J.* **2008**, *275*, 753 – 762.
[9] N. LeMaitre, W. Sougakoff, C. Truffot-Pernot, V. Jarlier, *Antimicrob. Agents Chemother.* **1999**, *43*, 1761 – 1763.
[10] M. M. Harding, *Acta Crystallogr. Sect. D* **2001**, *57*, 401 – 411.
[11] P. K. Fyfe, S. L. Oza, A. H. Fairlamb, W. N. Hunter, *J. Biol. Chem.* **2008**, *283*, 17672 – 17680.
[12] H. C. Pace, C. Brenner, *Genome Biol.* **2001**, *2*, 1 – 9.
[13] A. C. Storer, R. Ménard, *Methods Enzymol.* **1994**, *244*, 486 – 500.
[14] W. L. DeLano, *The PyMOL Molecular Graphics System*, DeLano Scientific, San Carlos, CA, USA, **2002**.